



NIH Public Access

Author Manuscript

Biochemistry. Author manuscript; available in PMC 2013 August 21.

Published in final edited form as:
Biochemistry. 2012 August 21; 51(33): 6511–6518. doi:10.1021/bi3002538.

Adhesion of Mussel Foot Protein Mefp-5 to Mica: An Underwater Superglue†

Eric W. Danner^{1,‡}, Yajing Kan^{2,3,‡}, Malte U. Hammer^{3,4}, Jacob N. Israelachvili³, and J. Herbert Waite^{1,*}

¹Molecular Cell and Developmental Biology Department, University of California, Santa Barbara, CA 93106

²Jiangsu Key Laboratory for Design and Manufacture of Micro-Nano Biomedical Instruments, Southeast University, Nanjing, China 211189

³Department of Chemical Engineering, University of California, Santa Barbara, CA 93106

⁴Centre for Innovation Competence „plasmatis“, 17489 Greifswald and Leibniz Institute for Plasma Science and Technology (INP), 17489 Greifswald

Abstract

Mussels have a remarkable ability to attach their holdfast, or byssus, opportunistically to a variety of substrata that are wet, saline, corroded, and/or fouled by biofilms. *Mytilus edulis* foot protein-5 (Mefp-5) is one of several proteins in the byssal adhesive plaque of the mussel *M. edulis*. The high content of 3,4 dihydroxyphenylalanine (Dopa) (~30 mol%) and its localization near the plaque-substrate interface have often prompted speculation that Mefp-5 plays a key role in adhesion. Using the surface forces apparatus, we show that on mica surfaces Mefp-5 achieves an adhesion energy approaching $E_{ad} = \sim 14 \text{ mJ/m}^2$. This exceeds the adhesion energy of another interfacial protein, Mefp-3, by a factor of 4–5 and is greater than the adhesion between highly oriented monolayers of biotin and streptavidin. The adhesion to mica is notable for its dependence on Dopa, which is most stable under reducing conditions and acidic pH. Mefp-5 also exhibits strong protein-protein interactions with itself as well as with Mefp-3 from *M. edulis*.

Adhesive plaque formation in the byssus of marine mussels (*Mytilus* sp.) represents a revealing case of how living organisms depend on and interact with inert materials in their habitats. Mussel adhesion is increasingly investigated to discover the biochemical and biophysical adaptations necessary for opportunistic and durable adhesion to solvated and moist mineral and metal oxide surfaces. Adhesive plaques contain as many as ten different proteins, known as *M. edulis* foot proteins (Mefps) that are distinguished by their basic isoelectric points and 3,4-dihydroxyphenylalanine (Dopa) content. Serial plaque sections reveal a Dopa gradient in which Dopa increases from below 2 mol% at the thread-plaque juncture to nearly 20 mol% in the plaque footprint¹. The gradient has prompted speculation that a high density of Dopa side-chains favors adhesion to wet surfaces. This view gained considerable weight by the AFM demonstration that a single tethered Dopa binds to wet

†This work was supported in part by the National Institutes of Health (R01 DE018468), Materials Research Science and Engineering Centers Program of the National Science Foundation under Award No. DMR 1121053 and China Scholarship Council.

*Author Email Address (waite@lifesci.ucsb.edu); Phone: 805-893-2817.

‡These authors contributed equally.

Supporting Information: Figures of Mefp-5 hydrophathy plot (S1), effects of salt concentrations (S2), a plot of total contact time vs. adhesive force (S3), effect of pH 7.5 on Mefp-5 adhesion (S4), and calculations of refractive index, protein volume fraction (S5), and strength of Dopa's H-bonds are available (S6) free of charge via the Internet at <http://pubs.acs.org>.

titania surfaces reversibly with a detachment force of nearing 1 nN² and that synthetic polymers functionalized with Dopa mimics increase adhesive strength to titania surfaces in proportion to their mol% of Dopa^{3,4}. As with other biomolecular adhesive systems e.g. cadherin^{5,6}, introduction of the surface forces apparatus (SFA) for investigating mussel adhesive proteins has enabled the precise, sensitive, and highly reproducible analysis of adhesive properties of purified Mfps taken individually or in combination^{7–10}.

Mussel foot protein-5 (Mefp-5) is small (10 kDa) and distinct from other Mfps by a 30 mol % Dopa content as well as high glycine (15 mol%) and lysine (17 mol%)^{11,12} (Figure 1). The basic residues are partially counteracted by glutamic acid and phosphoserine modifications. This collection of amino acids produces a very hydrophilic protein as seen in the hydropathy plot in Figure S1. Mefp-5 is present in small amounts in the byssal adhesive plaque where, together with Mefp-3, it is detectable by matrix-assisted laser desorption-ionization (MALDI) at the interface with the substrate surface¹¹. However, Mefp-5 requires rather higher laser power than Mefp-3 to be desorbed and ionized from surfaces during *in situ* footprint analysis by MALDI TOF mass spectrometry¹¹.

Here we report on our investigation of the attractive forces and work of adhesion between thin films of purified Mefp-5 and mica under buffered aqueous conditions. More specifically we explore the effects of changing pH, salinity, and redox on adhesion and cohesion. The results support the conclusion that Mefp-5 is the most adhesive protein of the Mfps tested to date; however, its adhesion, at least to mica, is highly reliant on low pH and the absence of oxidants.

Materials and Methods

Extraction of Mfps

Although methodology for the purification of Mefp-5 has been previously reported¹², the following adaptation was introduced to improve yields. Phenol glands from *Mytilus edulis* (L. 1758) feet were removed in batches of 150 as follows¹²: a pooled harvest of glands weighing 5–10g was prepared by successive extraction using two buffer treatments - A) 5% acetic acid with protease inhibitors (1 µM leupeptin and pepstatin and 10 mM EDTA) and B) 5% acetic acid and 8 M urea. Treatment A was used at a volume to initial wet weight ratio of about 10 mL/g and treatment B was performed at 7 mL/g pellet. All steps were performed in an ice bath using a frosted 35mL glass tissue grinder (Kontes Inc, Vineland, NJ) and followed by centrifugation at 5°C at 40,000g for 45 minutes. The pellet from treatment A was then subjected to treatment B. 33% w/v ammonium sulfate was added to the supernatant from treatment B, stirred for 30 min and the precipitate removed by centrifugation at 5°C at 40,000g for 45 min. The supernatant was then collected and dialyzed first by with 4L of 0.1% perchloric acid (PCA) and then in 0.1M borate, pH 8.2, in tubing with a molecular weight cutoff of 1,000 (Spectrum Industries, Los Angeles). Dialysis resulted in protein precipitation, which was collected by centrifugation at 40,000g for 45 min. Separation of proteins recovered from the pellet was then achieved with HPLC and Shodex chromatography. Purified proteins were identified by routine electrophoresis on acid-urea polyacrylamide gels (5% acetic acid and 8M urea)¹³ and staining with nitroblue tetrazolium (NBT)¹⁴. Further checks were carried out by amino acid analysis on a Beckman System 6300 Auto Analyzer as described previously¹⁵ and on MALDI using α-cyano-4-hydroxycinnamic acid as matrix. Extractions and isolation of Mefp-3 were done as described previously¹⁶.

Surface Force Apparatus

The surface forces apparatus (SurForce, SFA 2000, Santa Barbara, Ca) was used to measure the normal force-distance profiles. The design and technical details of this apparatus are reported elsewhere^{17,18}. Here, distance $D=0$ denotes the distance measured at flat contact of two freshly cleaved mica surfaces. After this, Mefp proteins were adsorbed to one or both mica surfaces from 0.1M acetic acid buffer (HAc) as dictated by the experimental configuration: 1) in the asymmetric set-up, a 20 μl droplet of 20 $\mu\text{g}/\text{ml}$ Mefp-5 was placed on the lower surface and a bare, freshly cleaved mica upper disc to measure the Mefp-5/mica adhesive interaction; 2) in the symmetric configuration, 20 μl of 60 $\mu\text{g}/\text{ml}$ Mefp-5 was applied to both lower and upper surfaces to measure the Mefp-5/Mefp-5 cohesive interaction force; 3) finally, with different Mefp films on both surfaces, 20 μl of 15 $\mu\text{g}/\text{ml}$ Mefp-5 on the lower surface and 20 μl of 20 $\mu\text{g}/\text{ml}$ Mefp-3 on the upper surface to measure the Mefp-5/Mefp-3 interactions. After a 20 min adsorption, the surfaces were rinsed with 3ml 0.1M HAc. Following positioning into the SFA, the surfaces were brought almost into contact with a droplet of buffer solution providing a bridge between the two surfaces. To keep the buffer droplet from evaporating, a second droplet of buffer was placed in the box to maintain the vapor pressure. The influence of pH and salt were investigated by flushing the droplet (~100 μL) with an excess of the new treatment buffer (3ml). Treatment buffers were 1) 0.1M HAc, pH 2.6, 0.1M KNO₃, 2) 0.1M Na acetate, pH 5.5 and 3) 0.1M acetic acid, pH 2.6, (and 0.05M, 0.1M or 0.3M KNO₃ for varying ionic strength). Periodate oxidation experiments were performed in 0.1M acetic acid, pH 3, 0.1M KNO₃ buffer with 0.2–1 nmol NaIO₄ added to induce oxidation. A pair of mica sheets with or without Mefp-5 films were then brought into contact using the motor drive and left unperturbed for a set time (“wait time”) before the motor reversed thereby applying a separation force of but a few nm/s - a rate slow enough to measure equilibrium conditions. The total contact time refers to the time from initial contact between the two surfaces to the final jump out, and includes the wait time for which the motor is paused. The experiments described here involved trials that were reproducibly repeated two or more times. In instances of buffer change, the pH was monitored with pH strips before and after the buffer replacement. Pure water (Millipore) was used for the preparation of all solutions and cleaning processes. Measured adhesion forces, F_{ad} , taken at the point before the jump out (D_j) are related to the adhesion energy per area (E_{ad}) according to JKR theory ($F_{ad} = 1.5\pi R * E_{ad}$) for deformable surfaces¹⁹, where R is the radius of contact.

Results

Adhesive Mefp-5/Mica Interactions

Mefp-5's high Dopa content of ~30 mol% and localization at plaque-substrate interface has provoked considerable interest in the adhesive properties of both the native form² and recombinant analogs²⁰. The surface forces apparatus (SFA), an instrument that measures interaction forces between two surfaces with nano-Newton force and Å distance resolution, was used to determine adhesion of Mefp-5 to mica. In asymmetric testing, a thin film of Mefp-5 was deposited onto a freshly cleaved mica surface, whereas the other mica surface was left untreated (Figure 2). The two surfaces were then brought together and held in contact for a predetermined wait time before a separation force was applied. The results show several trends. First, the approach (in-run) is distinctive for its “jump-in”. Data are collected at a constant rate and so an increase in distance between points on the in-run indicate an accelerated approach. Acceleration occurs in the 2–12 nm distance range (blue arrow). At a distance of ~1 nm, the proximity of the mica surfaces becomes limiting regardless of the applied compressive force; this limit is referred to as the hard wall. The hard wall is 1 nm greater than the approach of the two untreated mica surfaces and thus represents the hydrodynamic diameter of the compressed mica-bound Mefp-5 proteins.

Reversal of the motor drive imposes a gradually increasing separation force on the mica/Mefp-5 sandwich up to adhesive failure at D_f , and the surfaces quickly separate with a jump-out. Jump-outs in the SFA indicate either protein-mica (adhesive) breaks or protein-protein (cohesive) detachment if the films contain multiple layers. The adhesion of freshly prepared Mefp-5 at pH 2.6 and ionic strength of $I = 0.1\text{M}$ was instantaneous, with an initial $E_{ad} \sim 9\text{ mJ/m}^2$. The E_{ad} increased to -13.7 mJ/m^2 after a 1 h contact time (Figure 2).

Cohesive Strength

To assess the cohesive behavior of Mefp-5, a thin layer of Mefp-5 was deposited symmetrically on both mica surfaces. At low pH and ionic strength, the E_{ad} to separate the plates was around -2 mJ/m^2 and the hard wall was 3–4 nm (Figure 3). Notably, depositing a range of Mefp-5 concentrations (20–60 $\mu\text{g/ml}$) on both mica surfaces had a negligible effect on the average hardwall thickness of $\sim 5\text{ nm}$ (data not shown).

Effects of pH and Salt on Cohesion

Given the limited Mefp solubility and its susceptibility to oxidation at pH 7 (Fig S4), surface forces measurements were performed using acidic buffers ($\text{pH } 3$) as these maximize Mefp solubility and minimize auto-oxidation. A recent report, however, has determined that solution conditions beneath a mussel's foot, during plaque formation are indeed distinctly acidic ($\text{pH } 5.5$) and have an ionic strength of about 80–90 mM⁸. Adhesion using asymmetric deposition of Mefp-5 on mica was thus tested at two acidic pHs at which the protein remained fully soluble. Adhesion was 3-fold higher at pH 2.6 than at pH 5.5 (Figure 4). The significant reduction in adhesion with increasing pH parallels a similar effect in Mefp-3^{9,10}. We proposed earlier that pH-dependent Dopa oxidation is responsible for the adhesion loss in Mefp-3. As observed in previous studies^{9,10}, the extent of Dopa oxidation occurring at pH 5.5 in the SFA was significantly higher than in bulk solution at the same pH. The role of Dopa was further investigated by periodate-triggered oxidations detailed below.

Two symmetric Mefp-5 films exhibited significantly lower attraction for one another following pH elevation from 2.6 to 5.5 after film deposition. The initial cohesion at pH 5.5 was $\sim 66\%$ of cohesion measured at pH 2.6 (Figure 5). However, when these thin films were left in contact overnight at pH 5.5, the separating E_{ad} increased fivefold to $\sim -10\text{ mJ/m}^2$ – a magnitude comparable only with the asymmetric interfacial Mefp-5-mica failure. In addition, a significant hardwall increase from the original 4 nm thickness to around 12 nm occurred even though the proteins remained under compression the entire time.

Effects of pH 7.5 on cohesion were also investigated (Figure 6). Initial cohesion at pH 2.6 was obliterated upon raising the pH to 7.5. However, after leaving the surfaces in contact overnight a strong separation force -4.1 mJ/m^2 was required, but was less than half that used to separate Mefp-5 films at pH 5.5 (Figure 5).

Ionic strength has little effect on interacting symmetric Mefp-5 films (Figure S2). In the range of ionic strengths from $I=0.05$ to $I=0.3\text{ M}$, interactions remained largely unchanged. The higher charge screening is apparent from the compression of the hardwall and from the decreased repulsive forces on the in-run.

Periodate Oxidation & Dopa in Adhesion and Cohesion

The suggestive correlation between Dopa oxidation and pH in Mefp-5 was more specifically explored using a chemical oxidant, sodium periodate. Periodate converts Dopa to Dopaquinone by a 2-electron oxidation^{9,21}. Because the auto-oxidation of Dopa to Dopaquinone is negligible at pH 2.6, it is possible to stoichiometrically titrate Dopa oxidation with periodate without introducing other pH-dependent changes such as the

charges on the mica surface and Mefp-5. Exposing the asymmetrically deposited Mefp-5 to 0.6 nmol of periodate effectively abolished adhesion (Figure 7).

Addition of periodate to symmetric films of Mefp-5 before the proteins are brought into contact also had a detrimental effect on the cohesiveness of the protein layers (Figure 8): the addition of 1 nmol periodate completely abolished any intermolecular cohesion between the films.

Mefp-3 and Mefp-5 Interactions

Mefp-3 and Mefp-5 are co-localized at the plaque interface¹¹ and hence our investigation examined intrinsic interactions between these two proteins. Mefp-3 and Mefp-5 were deposited as thin films on separate mica sheets. Upon Mefp-5-Mefp-3 contact, there was an instantaneous interaction of -1.5 mJ/m^2 - with the adhesion energy, E_{ad} , after 60 minutes reaching -3.1 mJ/m^2 (Figure 9).

Discussion

The functional byssal adhesion of mussels is ultimately a systems problem with multiple length scales that span from the molecular interactions at the plaque-substratum interface to the radial disposition of the threads relative to the living tissues of the mussel²². Assessing the adhesive capabilities of various mussel foot proteins at the plaque-substrate interface is challenging due to the number of proteins and complex inter- and intra-molecular interactions during plaque formation. The extreme polymorphism and post-translational processing of Mfps further complicate matters, e.g. Mefp-3 has >30 sequence variants. In the present study, we opted to simplify the analysis by isolating single protein variants from precursor stockpiles in the phenol gland of the mussel foot. Subjecting purified proteins to mechanical tests on the surface forces apparatus has revealed very specific and quantifiable information about the adhesive capabilities of Mefp-5 from *M. edulis*.

Mica was in part used as the substratum for adhesion because muscovite mica has a molecularly smooth surface and has been extensively tested with other Mfps enabling comparisons^{7–10}; but mica also has a surface chemistry relevant to rocks in the natural habitat of mussels²³. Given the limited solubility of Mefp-5 at neutral to seawater pH, the range of pH was restricted to 2.6 and 5.5 for testing. In fact, this range mimics the processing environment of a mussel's foot during plaque formation¹⁰, significantly retards auto-oxidation, as well as maximizing protein solubility.

The interfacial interactions between mica and Mefp-5 were determined by the approach and separation of asymmetrically configured surfaces during analysis by SFA (Figure 2). Adhesive failure during post-contact separation is confidently associated with the Mefp-5/mica interface because, with a protein film thickness of only 1 nm, the hardwall cannot be more than one Mefp-5 molecule thick. In addition, the flat well of the force-distance separation profile is diagnostic of an adhesive monolayer²⁴. Mefp-5 exhibits a large E_{ad} of $\sim -14 \text{ mJ/m}^2$ to mica at pH 2.6. Cohesion on symmetrically deposited surfaces is but a fraction of this value, e.g. -2.4 mJ/m^2 . In addition Mefp-5's adhesion is 5-fold greater than the largest measured adhesion energy for Mefp-3 and three times the strongest iron-mediated adhesion of Mfps (Table 1).

Intact Dopa residues are essential for effective mefp-5 adhesion to mica. A stepwise increase in buffer pH to 5.5 and 7.5 (Fig S4) or periodate treatment has primarily one effect on mefp-5 chemistry: Dopa is oxidized to Dopaquinone. And this change results in the abolition of adhesion in the SFA and an increased hardwall. The hardwall increase has been attributed to the effect that tautomerization of Dopaquinone to α, β -dehydroDopa has on the

protein backbone rigidification⁷. As Dopa is necessary for adhesion, a bidentate H-bond between the catecholic OH groups of Dopa and the surface siloxanes seems the only reasonable chemical basis for interaction. The binding of catechols to cristobalite (a crystalline silica surface covered in siloxyl groups very similar to mica) has been modeled using density functional theory²⁵. Accordingly, each of the two hydroxyls in each catechol moiety is able to make up to two H-bonds- one with the electronegative oxygen and the other with the positive hydrogen to the hydroxyls of the silicate. This can produce three or even four H-bonds between a single Dopa and the silica surface. Based on the refractive index of the compressed proteins layers during SFA runs¹⁸ it was possible to quantify the volumetric percent of mefp-5 in the compressed layer (the hardwall) at about 95% was found (S5). If one third of the Dopa residues in each Mefp-5 protein bind to each mica sheet, the E_{ad} at pH 2.6 would translate to about 56.94 kJ/mol per Dopa (or 18.98 kJ/mol per each H-bond if the Dopa makes 3 H-bonds), a reasonable estimate for an H-bond (S6).

The magnitude of the Mefp-5-mica interaction merits comparison with other ligand -protein complexes. The biotin-streptavidin interaction has one of the highest known binding free energies at 66 kJ/mol²⁶. Binding between the ligand and receptor, attached in highly oriented fashion to the upper and lower mica surfaces respectively, achieved an adhesion energy approaching -10mJ/m^2 as measured by the SFA²⁷. Notably the biotin- streptavidin system and Mefp-5-mica interactions (Figure 2) both exhibit distinctive square well potentials. Theory predicts square well potentials when one part of a high affinity complex is flexibly tethered (biotin, Mefp-5) whereas the other is rigidly attached (streptavidin, Mica)²⁴. It is tempting to envision Mefp-5 as evolutionarily adapted to bind the polysiloxane surface of clays (e.g. mica) as precisely as a receptor binds a ligand.

Given that Mefp-5 has 50% more Dopa than Mefp-3 but five times the E_{ad} may point to the importance of conformation and binding ability. It is established that antifreeze proteins²⁸ and osteocalcins²⁹ are precisely tailored to bind their specific crystalline substrates, with osteocalcin only obtaining a secondary structure upon binding hydroxyapatite²⁹. Within this context, it seems reasonable to propose that certain mussel adhesive proteins such as Mefp-5 may be specifically adapted to bind a crystal lattice on the surface of freshly cleaved mica. Further work is needed to more fully investigate this hypothesis. The kinetics of adhesion of Mefp-5 to mica is also quite remarkable with a measurable -9mJ/m^2 after a few seconds in contact; when plotted on a log/log scale, the strait line indicates a power-law relationship, with the slope of 0.10 that is reminiscent of sintering rates (Figure S3)³⁰⁻³². The rate of Mefp-5 adhesion is not the only characteristic that resembles sintering; the morphology of the byssal plaque ultrastructure also appears to recapitulate the melting of powders to make shapes³³.

Generally speaking, Mfp adhesion to mica, is not rigidly proportional to Dopa content (Table 1) suggesting that other factors may be needed to facilitate Dopa binding. The twenty residues of Dopa in Mefp-5 are distributed at roughly every third residue. The resulting virtual bond spacing between Dopa side chains is estimated at no more than 1.1 nm apart. Scrutiny of the approaching in-run (Figure 2) reveals a jump-in at ~ 12 nm suggesting that unbound lengths of the protein exist with the ability to assume extended conformations, that then bind and draw in the opposing mica surface. Evidently, not all the Dopa side-chains in adsorbed Mefp-5 are bound to a mica surface at any given time, and unbound catecholic moieties are available for bonding to other surfaces or for specific interactions with neighboring proteins.

Strong specific interactions between opposing Mefp-3 and Mefp-5 films are particularly interesting given the interfacial location of both proteins in the byssus. Previous studies showed Mefp-3 to be moderately adhesive on mica but incapable of significant binding to

Mefp-2, Mcfp-6 or even to itself^{8,10}. Molecules adapted for practical adhesion rarely function in isolation but interact to various degrees with other molecules present. The ability of Mefp-5 to bind Mefp-3, Mefp-2, as well as to itself, implicates it as a "mediator" of interfacial molecules and of how loads are shared/transferred between them. Intrinsic interactions between Mefp-5 and Mefp-3 may represent the first line of cohesion to be later strengthened by metal complexes and covalent cross-links as the byssus matures. The measured E_{ad} between Mefp-5 and Mefp-3 is very similar to the E_{ad} of Mefp-3 to mica (Table 1). Perhaps the interaction between Mefp-3 and Mefp-5 is even stronger than measured, with failure actually occurring at the Mefp-3/mica interface. Except for their dependence on Dopa, the basis for the intrinsic interactions between Mfps remains a fascinating mystery.

Oxidation of Dopa has the potential either to diminish or increase the strength of interactions between Mefp-5 proteins. In studies of symmetric Mefp-5 films, periodate oxidation prior to brief contact and separation eliminated all the protein-protein cohesion measured by the SFA suggesting that the reduced form of Dopa is indispensable for Mefp-5 cohesion in the short term. The failure of a cohesive cross-linking interaction between Mefp-5 films immediately following periodate may be related to needing a partner in close proximity. Symmetrically deposited Mefp-5 under auto-oxidizing conditions at pH 5.5 enabled successful pairing of cross-linking partners, but only after overnight contact (oxidation evident from hardwall increase as discussed below). As covalent cross-linking tends to shift the system's weakest point from cohesion to H-bonding at the protein/mica interface, the observed increase in adhesion to -10mJ/m^2 (approaching the mJ/m^2 values associated with the Mefp-5/mica interaction) is expected (Figure 5). This adhesion is 2-fold greater than the greatest previously measured intrinsic interaction between any other mussel foot proteins. The time dependence of increase is due to the need for specific cross-linking partners, e.g. Dopaquinone and another amino acid, to find one another in a conformation dependent manner. In synthetic constructs, Dopaquinone based cross-links only formed in ordered structures that brought Dopa and its coupling partner together³⁴.

For cohesion experiments at pH 7.5, the reaction environment is significantly changed compared with pH 5.5 (Figure 6). Histidine (pK_a 6.4) and lysine (pK_a 10.4) side-chain cross-linking reactivity increases as pH approaches and exceeds the pK_a ³⁷. The initial lack of cohesion and hard-wall change reflect the oxidation of Dopa. Then, after an overnight (12h) contact, adhesion increased to -4.1 mJ/m^2 . In a suggestive study by Liu et al³⁴, oxidation of Dopa to quinone at pH 7.0 in a polymer with spatially coupled Dopa-lysine or Dopa-histidine pairs led to the formation of covalent adducts between the amine and quinone. As Mefp-5 has ~20% lysine and 5% histidine, this covalent cross-linking was expected. The long contact times needed can be attributed to the reduced flexibility of the protein backbone⁹ as well as being ~4 pH units below the lysine (pK_a the deprotonated form necessary for reactivity). Mfp-5 cohesion at pH 7.5 was notably less (one third) than at pH 5.5. This could be due to differences in the type and/or number of cross-links across the interface. At low pH with I_3^- oxidants, mostly diDopa cross-links formed by Dopa semiquinone coupling in mfp-1.³⁸ In contrast, at higher pH, reaction of uncharged histidinyl and lysyl groups with Dopaquinone become favored kinetically.^{2, 34}

Dopa-based mussel adhesion is fascinating because the catecholic (reducing) and quinonic (oxidizing) chemistries of Dopa both contribute to the natural maturation of the byssal holdfast. How mussels choreograph this complex balancing act has profound implications for practical wet adhesion and merits closer examination. The present study has showcased how important catecholic chemistry is for the initial interaction of Mefp-5 with mica and other protein layers. Significant quantities of hydronium ions and/or antioxidants such as Mcfp-6 are required to sustain Dopa as a catechol¹⁰. More distant from the interface,

quinone derived cross-links involving Dopa residues³⁵ and thiol cysteines¹¹ are known to form in byssal plaques. The imidazoles of histidine and ε-amines of lysine may provide additional cross-linking partners^{34,36}. Not all pathways involving Dopaquinone have cross-linking consequences; Dopaquinone tautomerization to dehydroDopa, for example, can produce backbone rigidification⁹, which has been proposed to account for the hardwall increases (Figures 5 and 8) that have been observed in all SFA experiments involving Mfp oxidation^{9,10}. The specific binding, cross-linking, oxidation-induced rigidification, and differential Mfp-metal affinity⁸ within a complex multiprotein secretion raises the possibility that mussels have evolved mechanisms to choreograph these diverse functionalities in a directed, site- and time-specific manner.

Supplementary Material

Refer to Web version on PubMed Central for supplementary material.

Acknowledgments

We would like to thank Wei Wei for assistance in protein purification and Jing Yu for valuable conversations.

Abbreviations

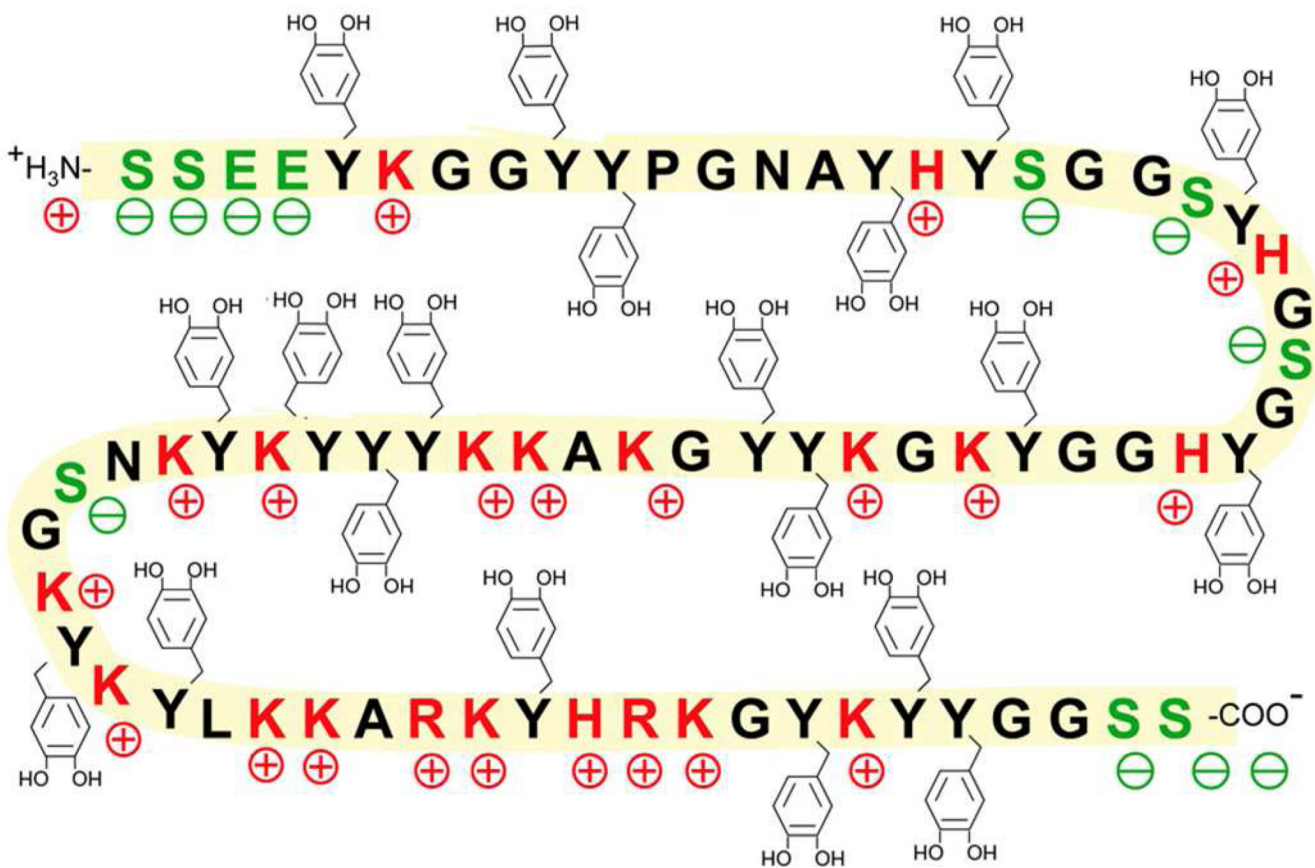
Mefp-5	<i>Mytilus edulis</i> foot protein 5
Mcfp-3	<i>Mytilus californianus</i> foot protein 3
Mfp	<i>Mytilus</i> foot protein
Mcfp-2	<i>Mytilus californianus</i> foot protein 2
Mcfp-6	<i>Mytilus californianus</i> foot protein 6
Dopa	3,4-dihydroxyphenylalanine
SFA	Surface Forces Apparatus
I	Ionic strength
AFM	atomic force microscopy

References

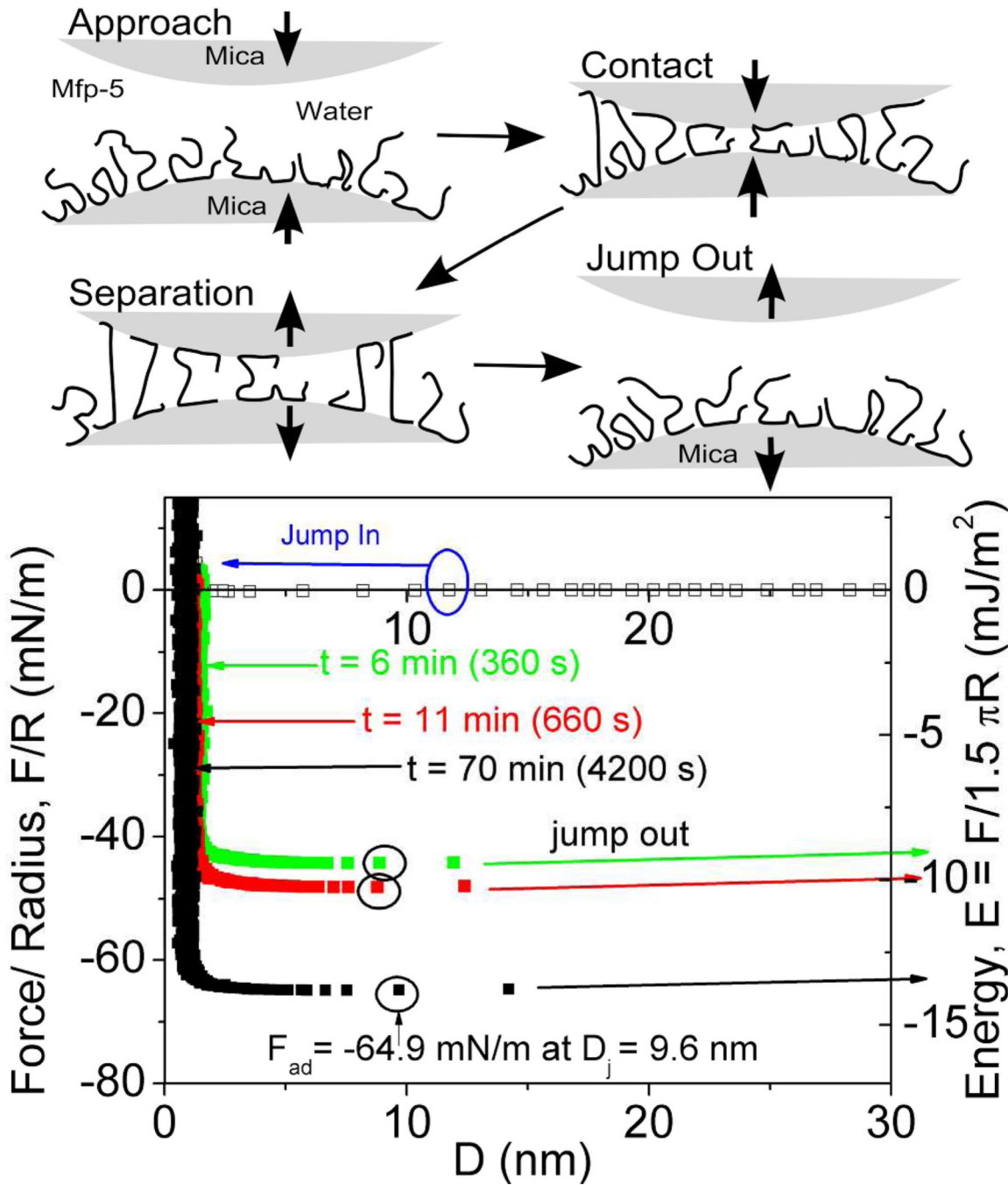
1. Rubin DJ, Miserez A, Waite JH. Diverse strategies of protein sclerotization in marine invertebrate structure–property relationships in natural biomaterials. *Adv. Insect Physiol.* 2010; 38:75–133.
2. Lee H, Scherer NF, Messersmith PB. Single-molecule mechanics of mussel adhesion. *Proc. Natl. Acad. Sci.* 2006; 103:12999–13003. [PubMed: 16920796]
3. Anderson TH, Yu J, Estrada A, Hammer MU, Waite JH, Israelachvili JN. The contribution of Dopa to substrate-peptide adhesion and internal cohesion of mussel-inspired synthetic peptide films. *Adv. Funct. Mater.* 2010; 20:4196–4205. [PubMed: 21603098]
4. Wang J, Tahir MN, Kappl M, Tremel W, Metz N, Barz M, Theato P, Butt HJ. Influence of binding-site density in wet bioadhesion. *Adv. Mater.* 2008; 20:3872–3876.
5. Sivasankar S, Brieher W, Lavrik N, Gumbiner B, Leckband D. Direct molecular force measurements of multiple adhesive interactions between cadherin ectodomains. *Proc. Natl. Acad. Sci.* 1999; 96:11820–11824. [PubMed: 10518534]
6. Bayas MV, Kearney A, Avramovic A, van der Merwe PA, Leckband DE. Impact of salt bridges on the equilibrium binding and adhesion of human CD2 and CD58. *Journal of Biological Chemistry.* 2006; 282:5589–5596. [PubMed: 17172599]

7. Lin Q, Gourdon D, Sun C, Holten-Andersen N, Anderson TH, Waite JH, Israelachvili JN. Adhesion mechanisms of the mussel foot proteins mefp-1 and mefp-3. *Proc. Natl. Acad. Sci.* 2007; 104:3782–3786. [PubMed: 17360430]
8. Hwang DS, Zeng H, Masic A, Harrington MJ, Israelachvili JN, Waite JH. Protein and metal-dependent interactions of a prominent protein in mussel adhesive plaques. *J. Biol. Chem.* 2010; 285:25850–25858. [PubMed: 20566644]
9. Yu J, Wei W, Danner E, Israelachvili JN, Waite JH. Effects of interfacial redox in mussel adhesive protein films on mica. *Adv. Mater.* 2011; 23:2362–2366. [PubMed: 21520458]
10. Yu J, Wei W, Danner E, Ashley RK, Israelachvili JN, Waite JH. Mussel protein adhesion depends on interprotein thiol-mediated redox modulation. *Nat. Chem. Biol.* 2011; 7:588–590. [PubMed: 21804534]
11. Zhao H, Waite JH. Linking adhesive and structural proteins in the attachment plaque of *Mytilus californianus*. *J. Bio. Chem.* 2006; 281:26150–26158. [PubMed: 16844688]
12. Waite JH, Qin X. Polyphosphoprotein from the adhesive pads of *Mytilus edulis*. *Biochemistry*. 2001; 40:2887–2893. [PubMed: 11258900]
13. Waite JH, Benedict C. Assay of dihydroxyphenylalanine (Dopa) in invertebrate structural proteins. *Methods Enzymol.* 1984; 107:397–413. [PubMed: 6438444]
14. Paz M, Fluckiger R, Boak A, Kagan H, Gallop P. Specific detection of quinoproteins by redox-cycling staining. *J. Biol. Chem.* 1991; 266:689–692. [PubMed: 1702437]
15. Waite JH. Precursors of quinone tanning: Dopa-containing proteins. *Methods Enzymol.* 1995; 258:1–20. [PubMed: 8524142]
16. Papov V, Diamond T, Biemann K, Waite JH. Hydroxyarginine-containing polyphenolic proteins in the adhesive plaques of the marine mussel *Mytilus edulis*. *J. Bio. Chem.* 1995; 280:20183–20192. [PubMed: 7650037]
17. Israelachvili JN, Adams GE. Measurement of forces between two mica surfaces in aqueous electrolyte solutions in the range 0–100 nm. *J. Chem. Soc., Faraday Trans. 1.* 1978; 74:975.
18. Israelachvili J, Min Y, Akbulut M, Alig A, Carver G, Greene W, Kristiansen K, Meyer E, Pesika N, Rosenberg K, et al. Recent advances in the surface forces apparatus (SFA) technique. *Rep. Prog. Phys.* 2010; 73:36601–36616.
19. Johnson KL, Kendall K, Roberts AD. Surface energy and the contact of elastic solids. *Proc. R. Soc. Lond. A.* 1971; 324:301–313.
20. Choi YS, Kang DG, Lim S, Yang YJ, Kim CS, Cha HJ. Recombinant mussel adhesive protein fp-5 (MAP fp-5) as a bulk bioadhesive and surface coating material. *Biofouling*. 2011; 27:729–737. [PubMed: 21770718]
21. Rzepecki LM, Waite JH. α,β -Dehydro-3, 4-dihydroxyphenylalanine derivatives: rate and mechanism of formation. *Arch. Biochem. Biophys.* 1991; 285:27–36. [PubMed: 1899328]
22. Lee BP, Messersmith PB, Israelachvili JN, Waite JH. Mussel-inspired adhesives and coatings. *Annu. Rev. Mater. Res.* 2011; 41:99–132. [PubMed: 22058660]
23. Chough, S.; Lee, H.; Yoon, S. *Marine Geology of Korean Seas*. 2nd ed. Amsterdam: Elsevier; 2000. p. 65–75.
24. Wong JY. Direct measurement of a tethered ligand-receptor interaction potential. *Science*. 1997; 275:820–822. [PubMed: 9012346]
25. Mian SA, Saha LC, Jang J, Wang L, Gao X, Nagase S. Density functional theory study of catechol adhesion on silica surfaces. *J. Phys. Chem. C.* 2010; 114:20793–20800.
26. Guo S, Ray C, Kirkpatrick A, Lad N, Akhremitchev B. Effects of multiple-bond ruptures on kinetic parameters extracted from force spectroscopy measurements: revisiting biotin-streptavidin interactions. *Biophys. J.* 2008; 95:3964–3976. [PubMed: 18621812]
27. Helm CA, Knoll W, Israelachvili JN. Measurement of ligand-receptor interactions. *Proc. Natl. Acad. Sci.* 1991; 88:8169–8173. [PubMed: 1896465]
28. Garnham C, Campbell R, Davies P. Anchored clathrate waters bind antifreeze proteins to ice. *Proc. Natl. Acad. Sci.* 2011; 108:7363–7367. [PubMed: 21482800]
29. Hoang Q, Sicheri F, Howard A, Yang D. Bone recognition mechanism of porcine osteocalcin from crystal structure. *Nature*. 2003; 425:977–980. [PubMed: 14586470]

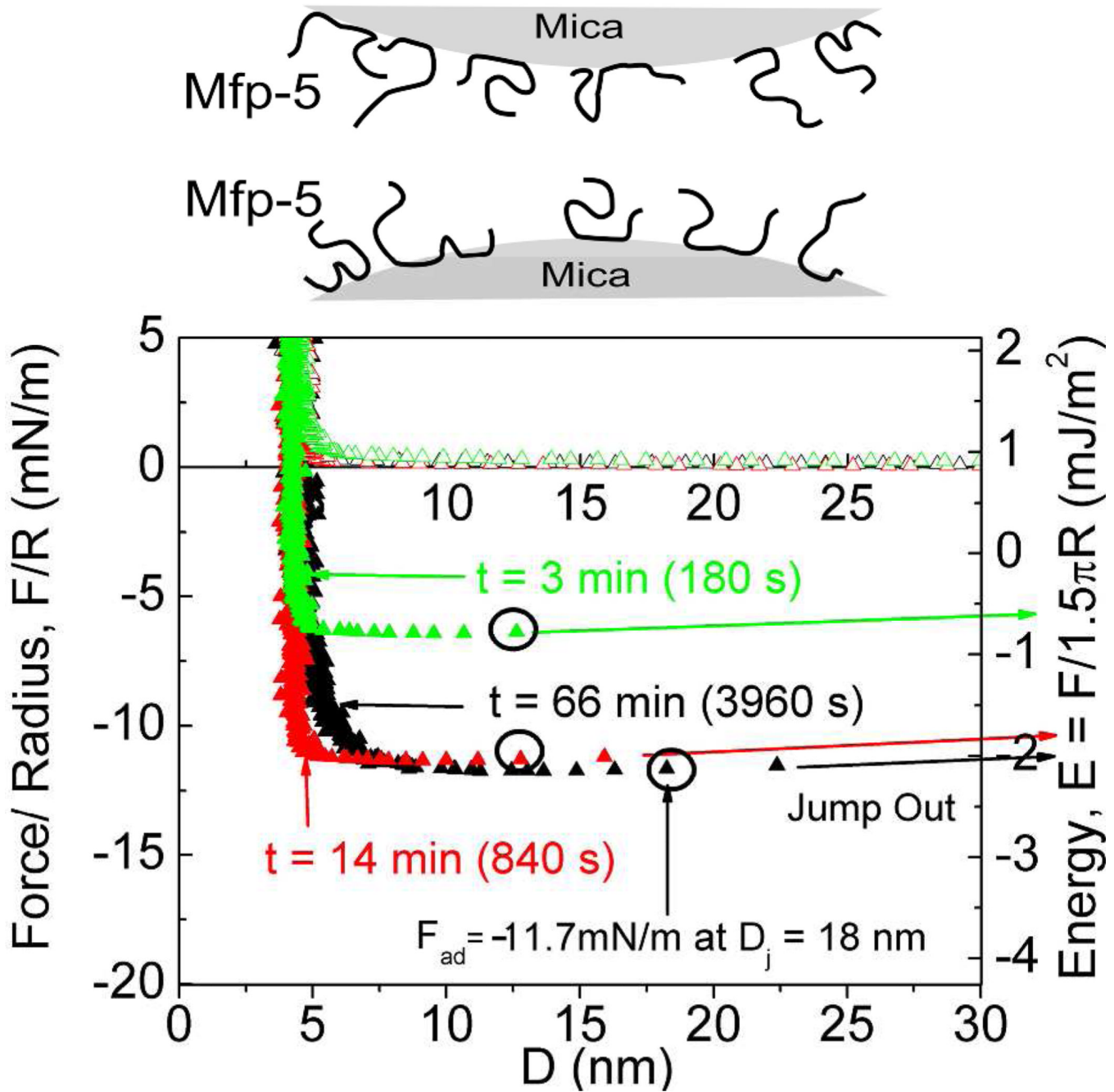
30. Vigil G, Xu Z, Steinberg S, Israelachvili J. Interactions of silica surfaces. *J. Colloid Interface Sci.* 1994; 165:367–385.
31. Exner H. Principles of single-phase sintering. *Rev. Powder Metall. Phys. Ceram.* 1979; 1:7.
32. German RM, Suri P, Park SJ. Review: liquid phase sintering. *J. Mater. Sci.* 2008; 44:1–39.
33. Benedict C, Waite JH. Composition and ultrastructure of the byssus of *Mytilus edulis*. *J. Morphol.* 1986; 189:261–270. [PubMed: 3772980]
34. Liu B, Burdine L, Kodadek T. Chemistry of periodate-mediated cross-linking of 3,4-dihydroxylphenylalanine-containing molecules to proteins. *J. Am. Chem. Soc.* 2006; 128:15228–15235. [PubMed: 17117875]
35. McDowell LM, Burzio LA, Waite JH, Schaefer J. Rotational echo double resonance detection of cross-links formed in mussel byssus under high-flow stress. *J. Biol. Chem.* 1999; 274:20293–20295. [PubMed: 10400649]
36. Miserez A, Rubin D, Waite JH. Cross-linking chemistry of squid beak. *J. Biol. Chem.* 2010; 285:38115–38124. [PubMed: 20870720]
37. Lee H, Rho J, Messersmith PB. Facile conjugation of biomolecules onto surfaces via mussel adhesive protein inspired coatings. *Adv. Mater.* 2009; 26:431–434. [PubMed: 19802352]
38. Haemers H, Koper GJM, Frens G. Effect of oxidation on cross-linking of mussel adhesive proteins. *Biomacromolecules.* 2003; 4:632–640. [PubMed: 12741779]
39. Zeng H, Hwang DS, Israelachvili JN, Waite JH. Strong reversible Fe³⁺-mediated bridging between Dopa-containing protein films in water. *Proc. Natl. Acad. Sci.* 2010; 107:12850–12853. [PubMed: 20615994]

**Figure 1.**

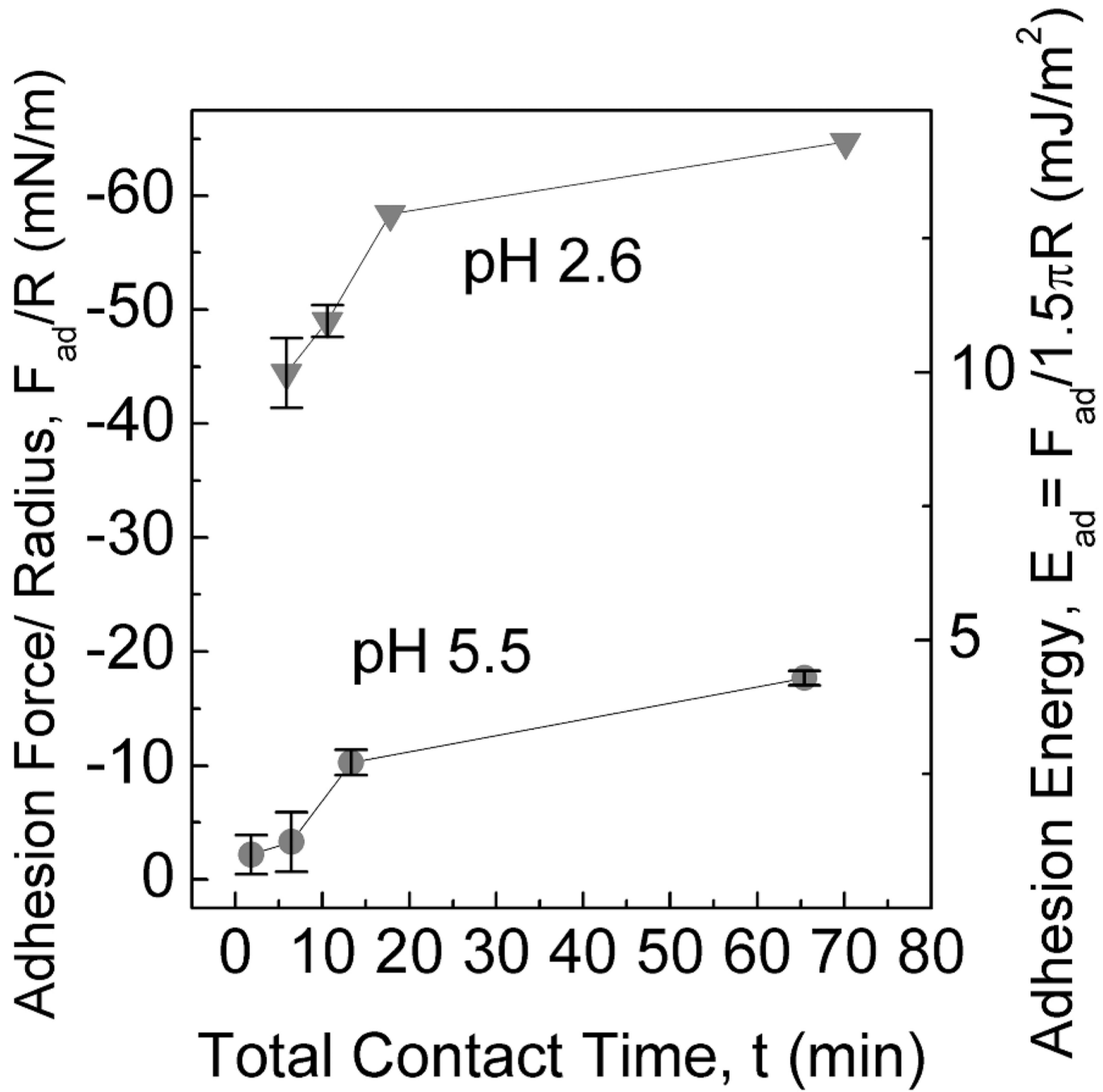
Sequence of Mefp-5. Red residues are positively charged, green residues are negatively charged and Dopa modifications (Y) are depicted with catecholic side chains. S denotes the location of phospho-Serine. Whereas the conversion of tyrosine to Dopa is complete in purified Mefp-5, the conversion of serine to phosphoserine is variable.

**Figure 2.**

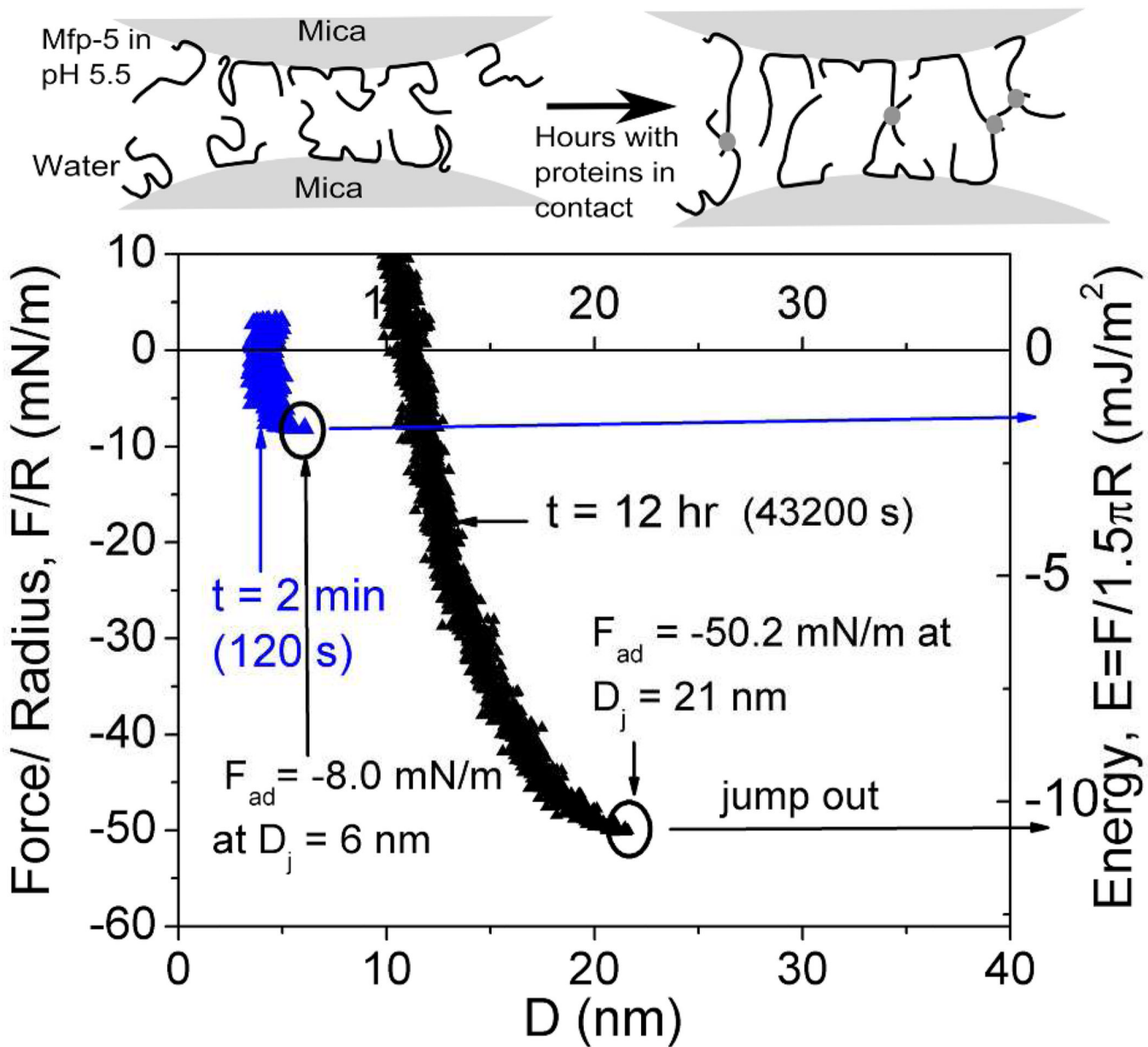
Mefp-5 interactions with mica as measured by the surface forces apparatus (SFA) with variable total contact times. Upper panels show how an asymmetric configuration with a Mefp-5 monolayer deposited on the lower mica surface and freshly cleaved mica on the upper surface was used to measure adhesion. Blue circle in the lower plot indicates beginning of jump-in; black circles denote F_{ad} for each run. Solution I=100mM, pH 2.6.

**Figure 3.**

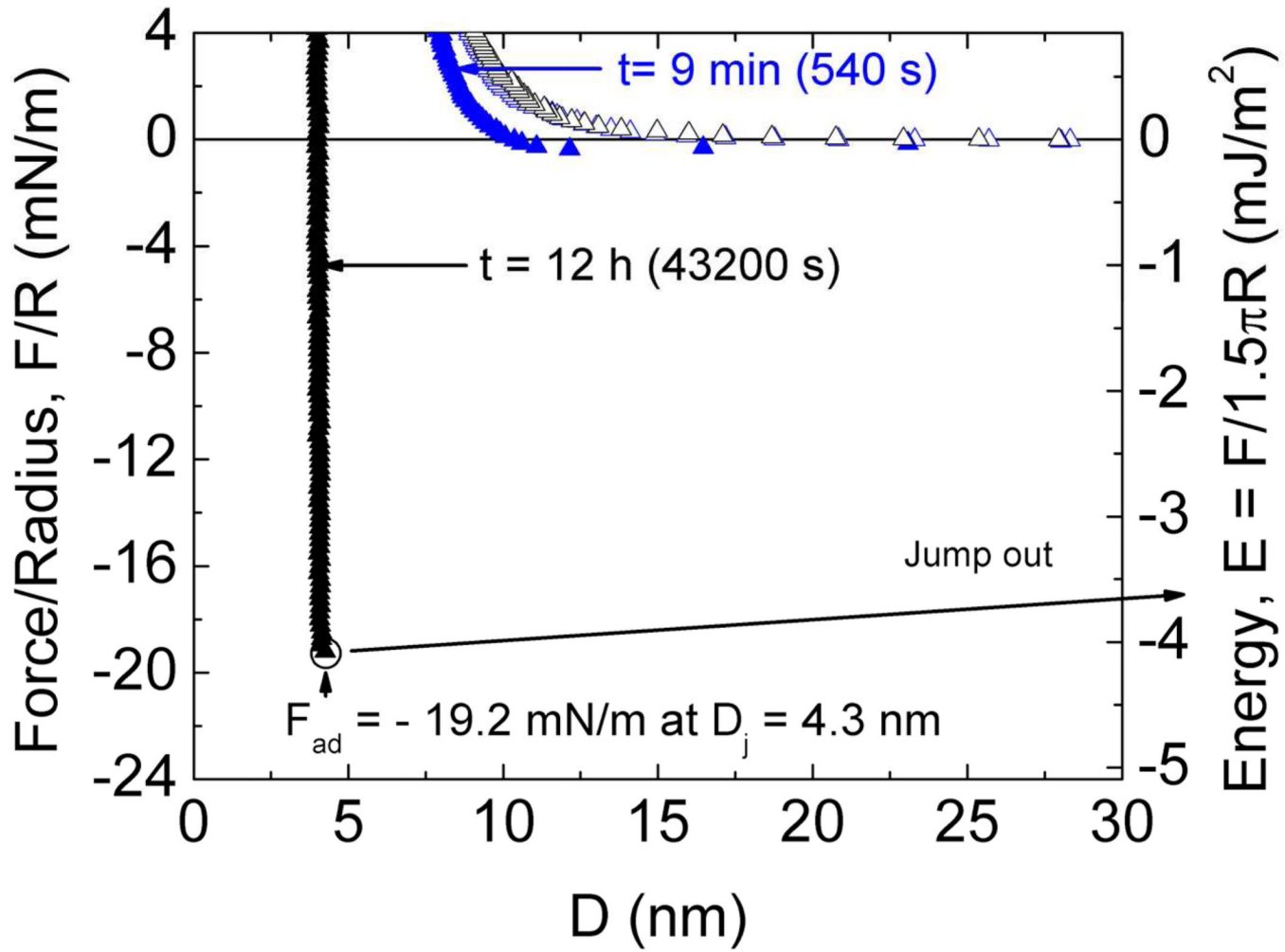
Mefp-5/Mefp-5 symmetric configuration with 20 μl of 60 $\mu\text{g/ml}$ protein deposited on both surfaces (schematic above graph) with 3 \times higher protein concentration during deposition than in other experiments. The total contact times are denoted with (t). Circled points indicate F_{ad} of the run. Solution I=100 mM, pH 2.6.

**Figure 4.**

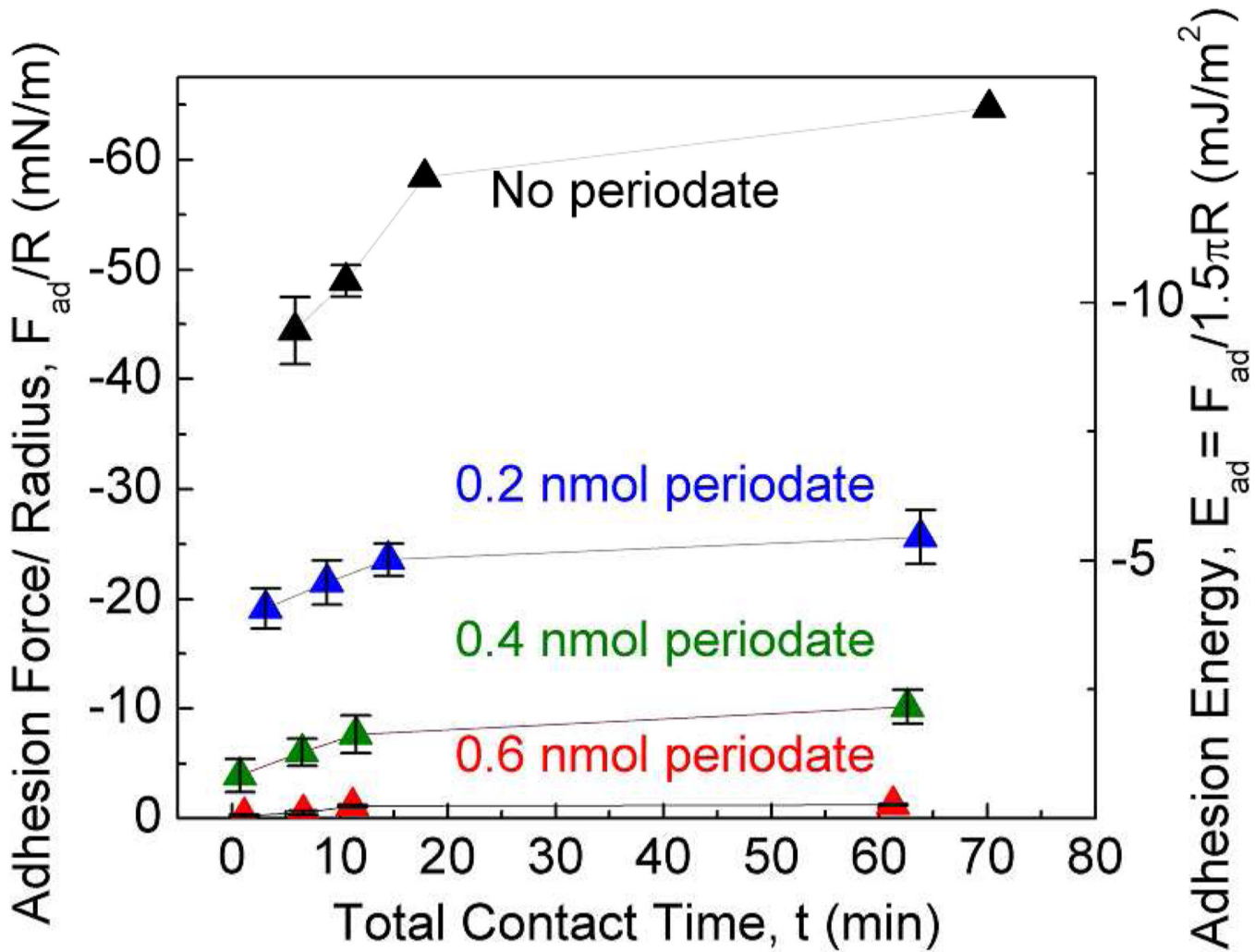
Effect of pH on peak adhesive force F_{ad} and adhesion energy E_{ad} between Mefp-5 and freshly cleaved mica surface (upper panel schematic). Results are plotted at pH 2.6 and 5.5 as a function of total contact times. Ionic strength is 100 mM. Error bars indicate standard deviation of at least two measurements.

**Figure 5.**

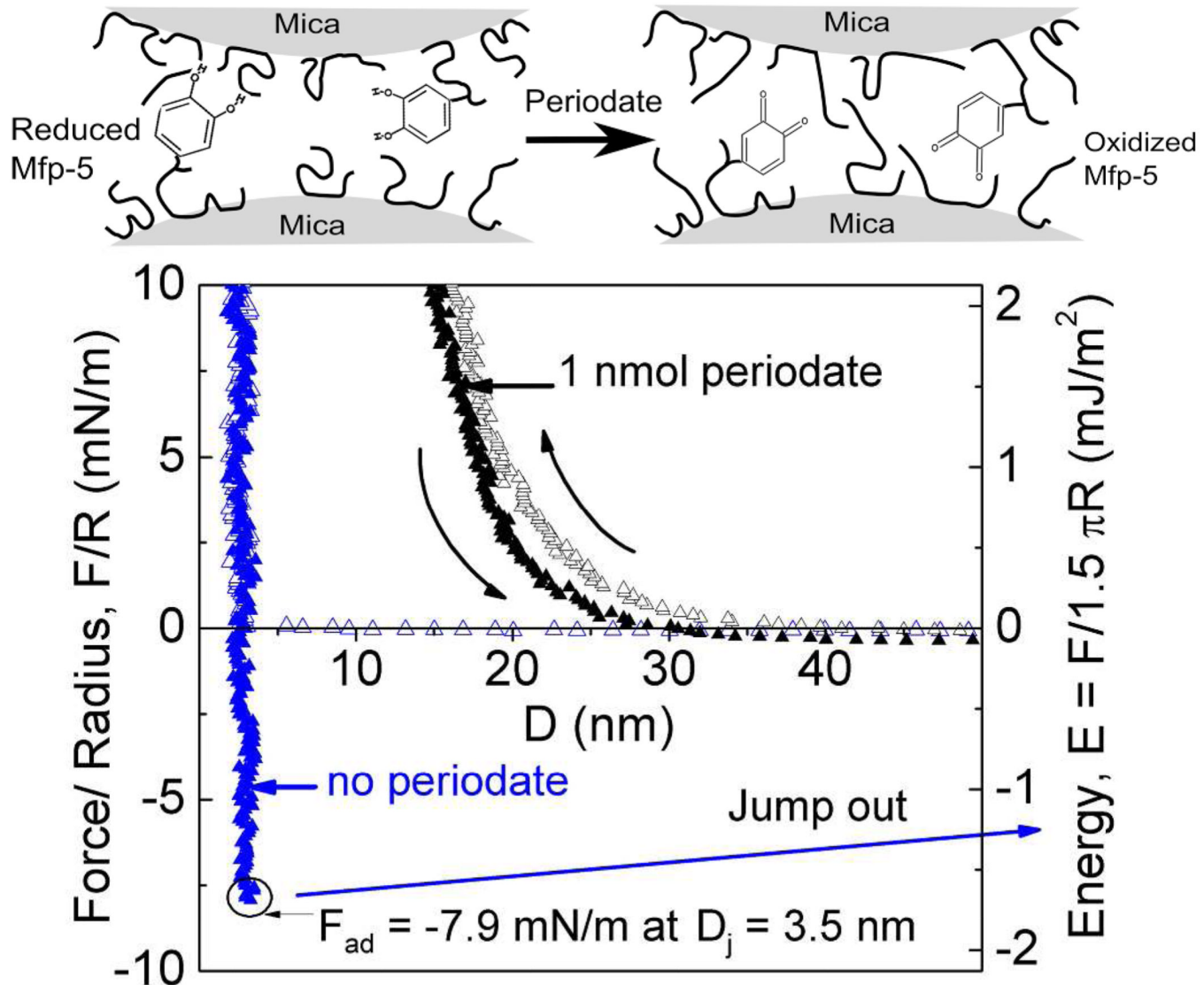
Effect of auto-oxidation on cohesion in symmetrically deposited Mfp-5 in at pH 5.5 and I=350 mM. After an initial short cohesion (blue), protein covered surfaces were left in contact in the auto-oxidizing solution for 12 hrs before separation (black). Upper panel depicts cross-link formation (dots) during contact following exposure to pH 5.5.

**Figure 6.**

Effect of auto-oxidation on cohesion in symmetrically deposited Mefp-5 in at pH 7.5 and I=234 mM. After the short-term contact (blue), protein covered surfaces were left in contact in the auto-oxidizing solution for 12 hrs before separation (black).

**Figure 7.**

Effect of Dopa oxidation by periodate treatment (upper panel) on peak F_{ad} and E_{ad} between Mefp-5 and mica at different total contact times before separation (lower panel). All runs were done at pH 2.6 and I=100 mM. Error bars indicate standard deviation of at least two measurements.

**Figure 8.**

Effect of periodate treatment on the cohesive interaction between symmetrically deposited Mfp-5 films taken after 12 minute (760 s) total contact times. Oxidation of Dopa to Dopaquinone by periodate treatment (upper panel) while protein films are separated abolishes cohesion (black), evident in the untreated controls (blue). pH 2.6 and I= 100 mM.

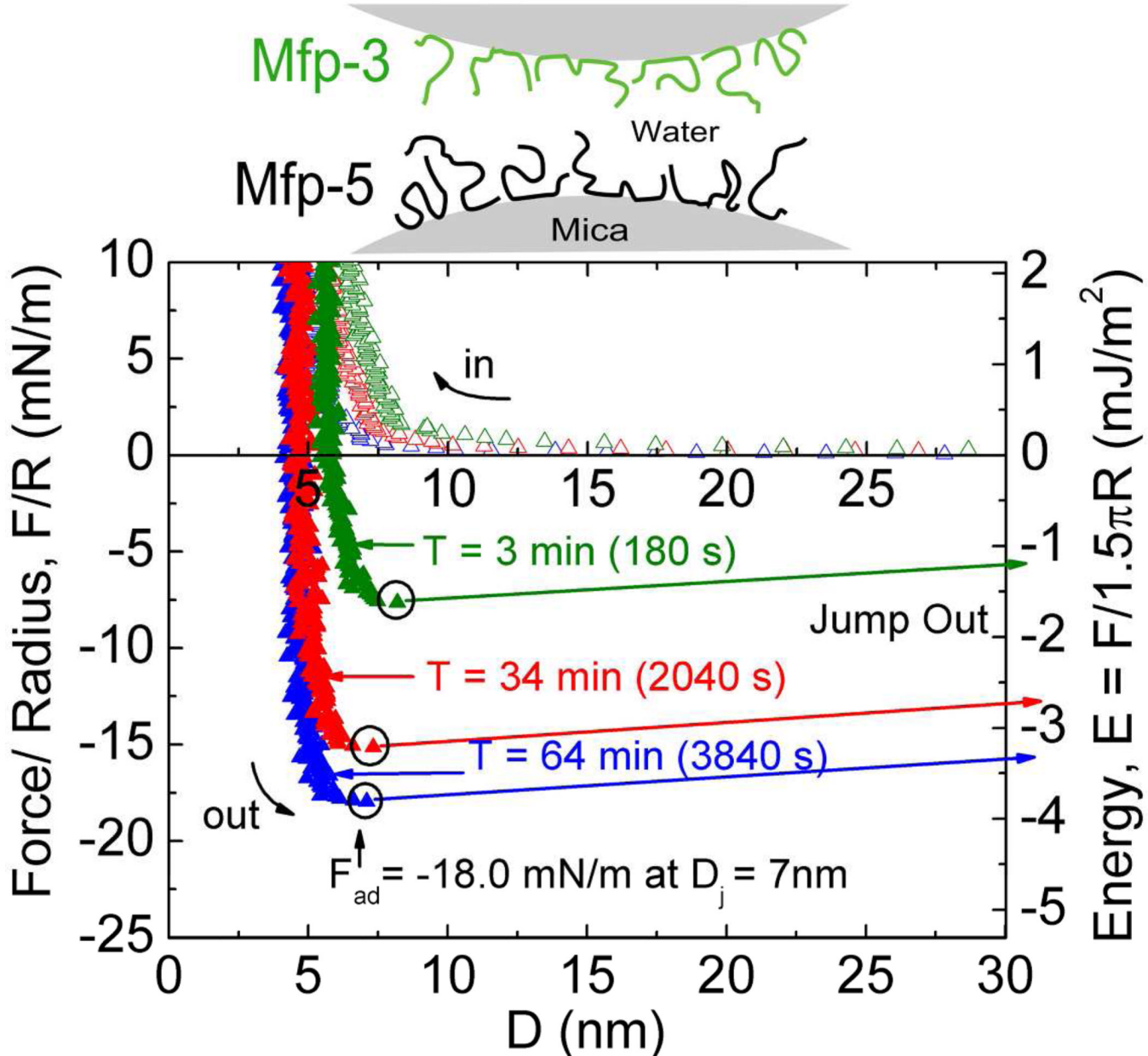


Figure 9.

Interaction between two interfacial plaque proteins, Mefp-3 and Mefp-5 with different total contact times. Mefp-3 and Mefp-5 monolayers were deposited asymmetrically on opposing mica surfaces (upper panel). Circled portions indicate F_{ad} for run. Solution pH 2.6 and $I=100$ mM.

Table 1

Summary of known *Mytilus* foot protein interactions as measured by SFA on mica.

Mussel foot protein	Dopa %	Adhesion energy, E _{ad} Asymmetric (mJ/m ²)	Adhesion energy, E _{ad} Symmetric (mJ/m ²)	Reference
Mefp-1	15	< -0.1	< -0.1	(7)
Mefp-2	5	< -0.1	< -0.1	(8)
Mcfp-3	20	-2.6		(9)
Mefp-3	20	-2.2		Unpublished
Mefp-4	2	< -0.1	< -0.1	Unpublished
Mefp-5	30	-13.7	-2.4	This work
Mcfp-6	3	< -0.5	< -0.5	(10)
Mefp-3 <-> Mefp-2	20/5	0		Unpublished
Mefp-3 <-> Mefp-5	20/30	-3.1		This work
Mefp-2 <-> Mefp-5	5/30	-1.4		(8)
Metal Mediated Interactions:				
Mefp-2 + Fe ³⁺	5		-2.2	(8)
Mefp-1 + Fe ³⁺	15		-4.3	(39)